Estimate MFE of secondary structure and thermodynamic Ensemble prediction of hsa-mir-181a ACE2 in un/vaccinated samples compared with the wild type

Mohammed. K. S. Alquraishi[1], Maha Mashrq Al-Bayati[2], Mustafa Hamza AlFatlawi[3], Noor Alamer[4], Mohammad Alzeyadi[5]

1- Assistant lecturer, Department of Pathological Analyses, Faculty of Science, University of Kufa, Iraq
2- Assistant lecturer, Department of Medical Laboratory Technology, Faculty of Medical Technology, University of Imam Jaafar Sadiq, Najaf, Iraq
3- Assistant lecturer, Department of Pathological Analyses, Faculty of Science, University of Kufa, Iraq
4- Assistant lecturer, Department of Pathological Analyses, Faculty of Science, University of Kufa, Iraq
5- Professor, Department of Biology, Faculty of Science, University of Kufa, Iraq

Received: January 12, 2024. Revised: May 9, 2024, Accepted: June 24, 2024.
DOI:10.21608/jbaar.2024.396492

Abstract

Using intelligent computer programs, the secondary structure and thermodynamic properties of hsa-mir-181a ACE2 were investigated in both vaccinated and unvaccinated samples, comparing them to the wild type. By utilizing the RNAalifold web server, a consensus structure of aligned micro-RNA sequences was predicted, along with the minimum free energy (MFE) and equilibrium base-pairing probabilities. The results showed a strong correlation between the secondary structure of hsa-mir-181a ACE2 and the vaccination status, with a higher MFE observed in the vaccinated group. This study proved a significant relationship between the secondary structure of hsa-mir-181a ACE2 and the selected class of vaccinated or unvaccinated. The value of (MFE) of the secondary structure of microRNA increased in vaccinated compared with unvaccinated, with a significant difference evident. Also, at the thermodynamic free energy (value) level, the vaccination was increased compared to the unvaccinated as the difference was clear and the relationship was achieved.

Keywords: MicroRNA, Computational microRNA, Minimum free energy, Thermodynamic free energy, The RNAalifold web server.

1. Introduction:

1.1 Micro RNA

Scientists have discovered miRNAs in a variety of living organisms, including animals, plants, and viruses, and there are undoubtedly more to be discovered. These small ~22-nt RNAs can induce mRNA degradation or translational repression through precise base pairing. Additionally, miRNAs can target multiple mRNAs, often working together with other miRNAs, thus creating intricate regulatory networks (1,2). Numerous studies have identified numerous microRNAs that are involved in the production of ACE2, with hsa-mir-181a being one of these. Additionally, some research suggests that the coronavirus family has gotten its paws into the expression of genes and genes themselves (3).

1.2 Genomic of Micro RNA

Except for the Y chromosome, miRNA genes are dispersed across the human genome. Half of the miRNAs that are now known to exist are transcribed as polycistronic main transcripts and are found in clusters. A gene cluster may be the consequence of gene duplication if the miRNAs

inside it are often connected to one another. Unrelated miRNAs are frequently found inside a miRNA gene cluster (4). Though plausible but unverified is the theory that the clustered miRNAs target different genes in the same pathway or the same gene, suggesting a functional connection between them (5).

1.3 Computational microRNA

Numerous computational approaches for predicting miRNA targets are centered on a few essential characteristics, including evolutionary conservation and complementarity to the 5′seed of miRNAs. Even while these characteristics make it possible to identify targets with success, not all miRNA target sites follow canonical seed complementarity and are preserved. The usage of mRNA: miRNA duplexes' energy properties as an alternate feature has been promoted by a number of research. Nonetheless, inconsistent findings regarding the validity of energy-based predictions for distinct genes within the same pathway were reported by several independent assessments (6).

In recent years, several new putative miRNAs have been identified in various species because of technological advancements like bioinformatics and next-generation sequencing (NGS). Estimating the overall number of miRNAs in humans and other animals is challenging (7).

1.4 Minimum free energy

Several computational methods have been created to forecast the secondary structure of RNA. Recent developments have been noteworthy for two of these techniques: Minimum Free Energy (MFE) and Maximum Expected Accuracy (MEA). This thesis has two key objectives: 1) to use constraint generation (CG) to estimate the free energy parameters, particularly for the MEA, and 2) to experimentally examine the accuracy (i.e., the quantity of base pairs in different energy models that the MFE and MEA algorithms correctly predict (8).

1.5 Thermodynamic free energy

A method for producing any suboptimal secondary structure between the lowest free energy and any upper bound is provided. When the algorithm is close to the lowest free energy, it operates very quickly. This permits the efficient approximation of statistical values, such as the partition function or measures for structural diversity. From a thermodynamic perspective, determining how well-defined the ground state is depends critically on the density of states at low energies and the structures that are connected with it (9).

1.6 The RNAalifold web server

For a group of related RNAs, predicting a consensus structure is a crucial initial step in further analysis. One of the first and most used tools for this endeavor is the RNA alifold, which calculates the minimal energy structure that is concurrently produced by a collection of aligned sequences. A number of other strategies have been promoted recently, highlighting various drawbacks of the first RNAalifold strategy (10).

2. Methods

Creating a predicted visualization of the consensus structure of the miRNAs hsa-mir-181a for both vaccinated and unvaccinated members of the miRNAs has-mir-181a class and using that consensus structure to match with the query sequence was the fundamental concept behind the present methodology. Using specialized software and websites, a set of data was extracted from pre-miRNA by converting total RNA to cDNA, reading the DNA sequence, and determining the in situ secondary structure of these sequences. The sequences were then compared with each other and with sequences that were available on the microRNA database website. The human miRNA classes that were available guided the selection of the data. 50 equal samples of vaccinated and non-vaccinated (11).

Samples Demographics

This research was done to examine fifty cases of humans (females and males 25 volunteers vaccinated and 25 volunteers unvaccinated who are from Najaf Governorate) all of whom were not previously infected with COVID-19. The ages of the volunteers ranged from 18 to 60 years.

Type of vaccine

For vaccinated people, the Pfizer vaccine was approved at a rate of more than 90%, with some of the rest of those who received the Sinopharm or BBIBP-CorV vaccine.

3. Results

3.1 MFE of secondary structure and thermodynamic ensemble prediction of hsa-mir-181a ACE2 in vaccinated samples.

The (MFE) to (RNAs) increases at an apparent linear rate with sequence length. To directly compare the folding stability of RNAs of different sizes, basic indices have been created by dividing the MFE by the total number of nucleotides. in this study, we achieved several results of MFE of secondary structure and thermodynamic ensemble prediction of hsa-mir-181a ACE2 in vaccinated samples comparative with the secondary structure of hsa-mir-181a ACE2 in wild type according to RNAalifold web server as shown in table 3.1.

Table 3.1. showing the (MFE) and the thermodynamic ensemble of the secondary structure of hsa-mir-181a ACE2 in vaccinated samples compared with the secondary structure of hsa-mir-181a ACE2 in wild type according to RNAalifold web server.

Vaccinated	(MFE) kcal/mole	Thermodynamic ensemble kcal/mole.	Vaccinated	(MFE) kcal/mole	Thermodynamic ensemble kcal/mole.
wild	**-53.70**	**-54.75**	**7**	**-38.00**	**-39.20**
1	**-41.81**	**-41.70**	**8**	**-44.00**	**-44.94**
2	**-42.80**	**-44.42**	**9**	**-49.40**	**-50.12**
3	**-43.70**	**-44.49**	**10**	**-48.80**	**-50.92**
4	**-42.10**	**-43.11**	**11**	**-48.10**	**-49.60**
5	**-49.10**	**-50.15**	**12**	**-28.60**	**-31.55**
6	**-47.10**	**-49.04**	**13**	**-29.90**	**-33.19**

The Graphical output of the secondary structure of *hsa-mir-181a ACE2* as described in Figure 3.1

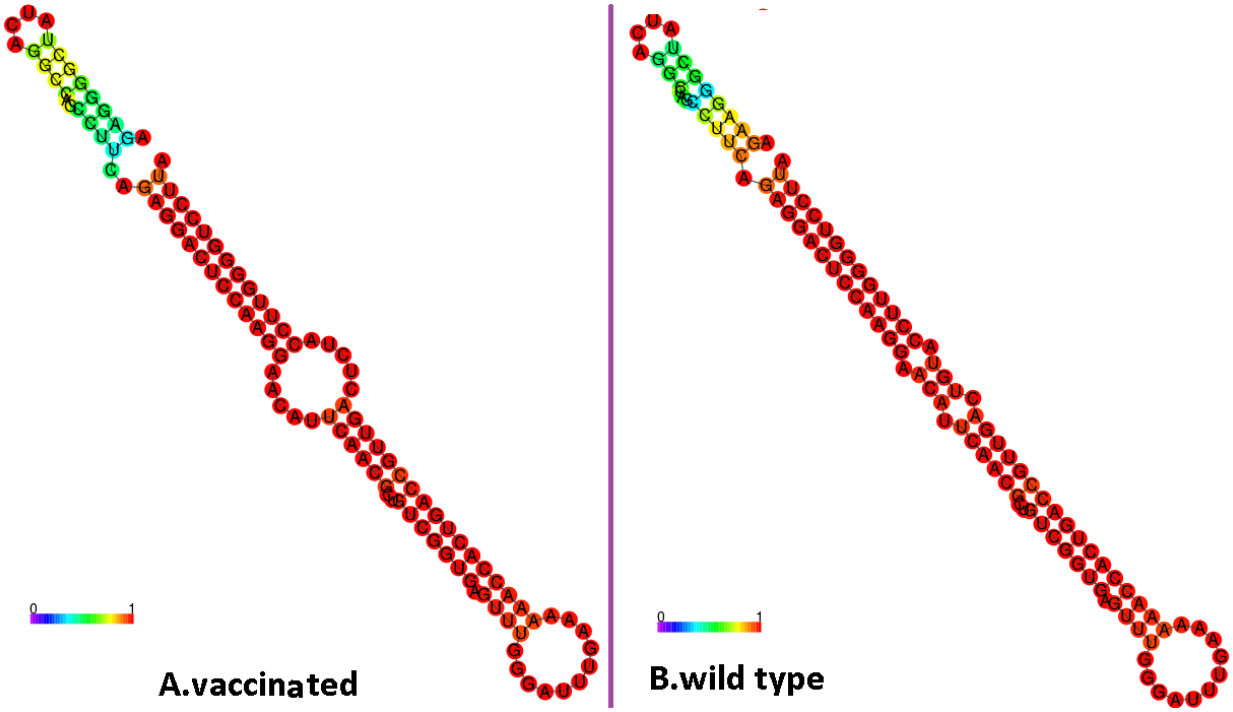

Figure 3.1 Base-pair probabilities are encoded from red 1% to purple 0% kcal/mol in the graphic representation of the secondary structure of hsa-mir-181a ACE2 found in the structure drawing. **A**. Sample 1 of vaccinated with a (MFE) of **-41.81**kcal/mole. **And** the thermodynamic ensemble is **-41.70** kcal/mole. **B**. Sample of wild type with a (MFE) **-53.70** kcal/mole. **The** thermodynamic ensemble is **-54.75** kcal/mole.

The largest change that occurred in the (MFE) of the vaccinated samples was in sample number 12 where was with a (MFE) of **-28.60** kcal/mole. **and** the thermodynamic ensemble is **-31.55** kcal/mole.

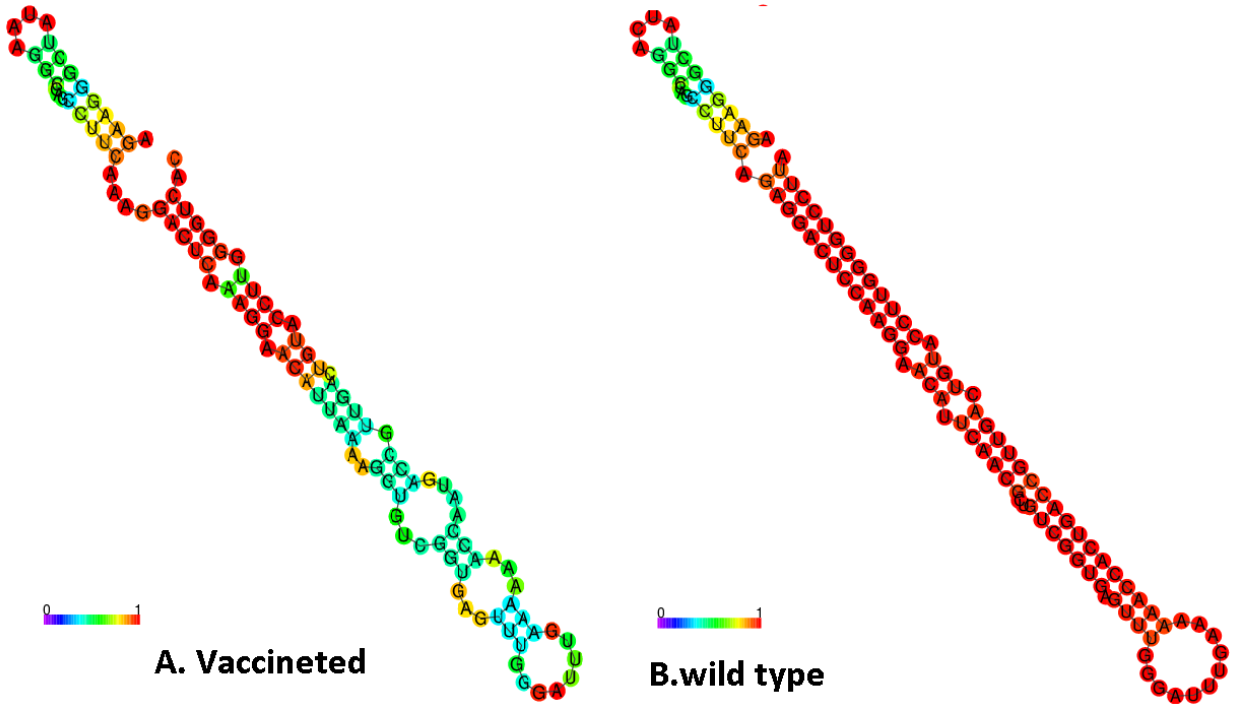

Figure 3.2 The Graphical drawing of the secondary structure of *hsa-mir-181a ACE2* as in structure drawing encoding base-pair probabilities from red 1% to purple 0% kcal/mol. **A**. sample 12 of vaccinated with a (MFE) of -**28.60** kcal/mole. The thermodynamic ensemble is -**31.55** kcal /mol. **B**. Sample of wild type with a (MFE) of -**53.70** kcal/mole. The thermodynamic ensemble is -**54.75** kcal/mole.

Optimal secondary structure in the dot-bracket notation of universal sequences of all micro-RNA sequences of 20 vaccinated samples as a multiple sequence alignment with a (MFE) of -**20. 31** (-**4.21** plus -**16.10** from covariance contributions) kcal/mole **and** the thermodynamic ensemble is -**23.36** kcal/mole is given below. Figure 3.3

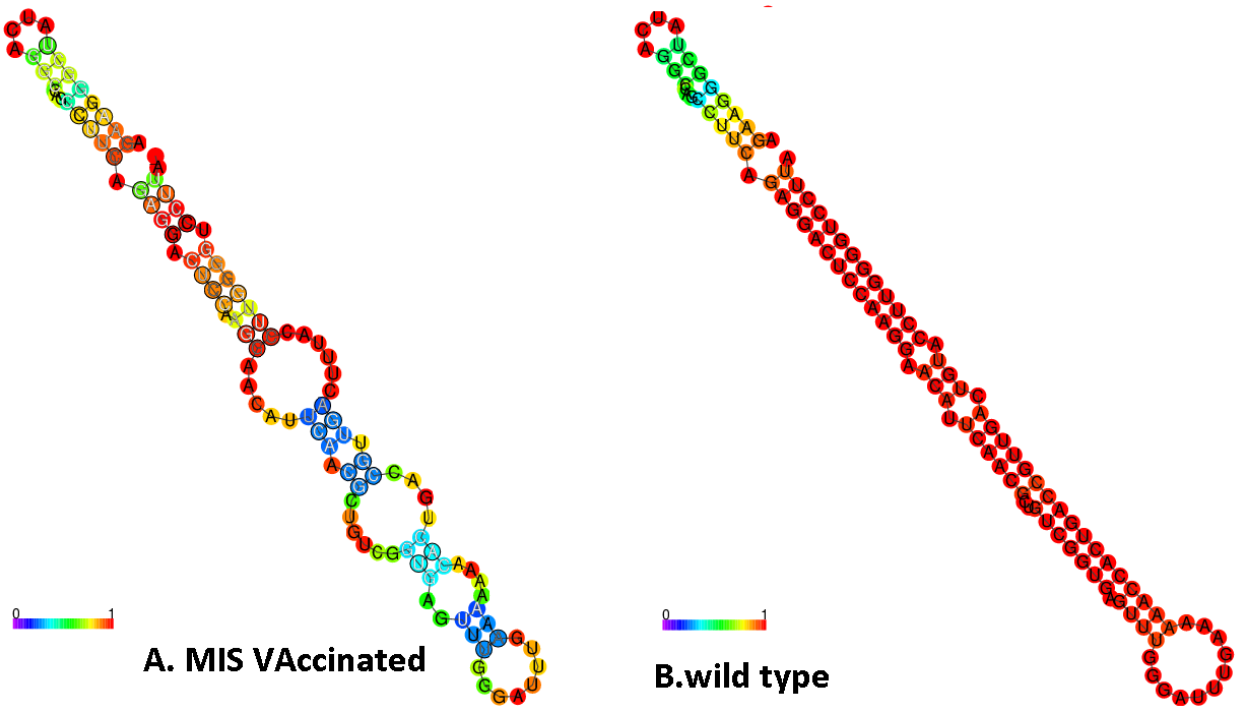

Figure 3.3 The secondary structure of hsa-mir-181a ACE2 is depicted graphically in the structure drawing, which encodes base-pair probabilities ranging from red (1% kcal/mol) to purple (0% kcal/mol). **A**. The multiple sequence alignment of all micro RNA sequences of 20 vaccinated samples with a (MFE) of -**20.31**kcal/mole. The thermodynamic ensemble is -**23.36** kcal /mole. **B**. Sample of wild type with a (MFE) of -**53.70** kcal/mole. The thermodynamic ensemble is -**54.75** kcal/mole.

3.2 MFE of secondary structure and thermodynamic ensemble prediction of hsa-mir-181a ACE2 in unvaccinated samples.

In this study, We achieved The MFE of secondary structure and thermodynamic ensemble prediction of hsa-mir-181a ACE2 in unvaccinated samples compared with the secondary structure of hsa-mir-181a ACE2 in wild type according to the RNAalifold web server as shown in table 3.2.

Table 3.2. Showing the (MFE) and the thermodynamic ensemble of the secondary structure of hsa-mir-181a ACE2 in unvaccinated samples comparative with the secondary structure of hsa-mir-181a ACE2 in wild type according to the RNAalifold web server.

Unvaccinated	(MFE) kcal/mole	Thermodynamic ensemble kcal/mole.	Unvaccinated	(MFE) kcal/mole	Thermodynamic ensemble kcal/mole.
wild	**-53.70**	**-54.75**	**7**	**-50.00**	**--51.29**
1	**-52.90**	**-53.88**	**8**	**-48.80**	**-50.18**
2	**-52.70**	**-53.24**	**9**	**-48.50**	**-48.96**
3	**-54.10**	**-54.94**	**10**	**-49.10**	**-50.07**
4	**-50.70**	**-52.18**	**11**	**-47.00**	**-47.63**
5	**-53.70**	**-54.75**	**12**	**--49.70**	**-50.62**
6	**-54.10**	**-54.94**	**13**	**-51.30**	**-52.30**

Table 3.3 The (MFE) and the thermodynamic ensemble of the secondary structure of hsa-mir-181a ACE2 in vaccinated samples compared with the secondary structure of hsa-mir-181a ACE2 in the wild.

Mean SD ±	**Vaccinated**	**Unvaccinated**	P. value ≤ 0.005
MFE (The minimum free energy)	-43.44	-51.03	

The Graphical output of the secondary structure of *hsa-mir-181a ACE2* is described in Figure 3.4.

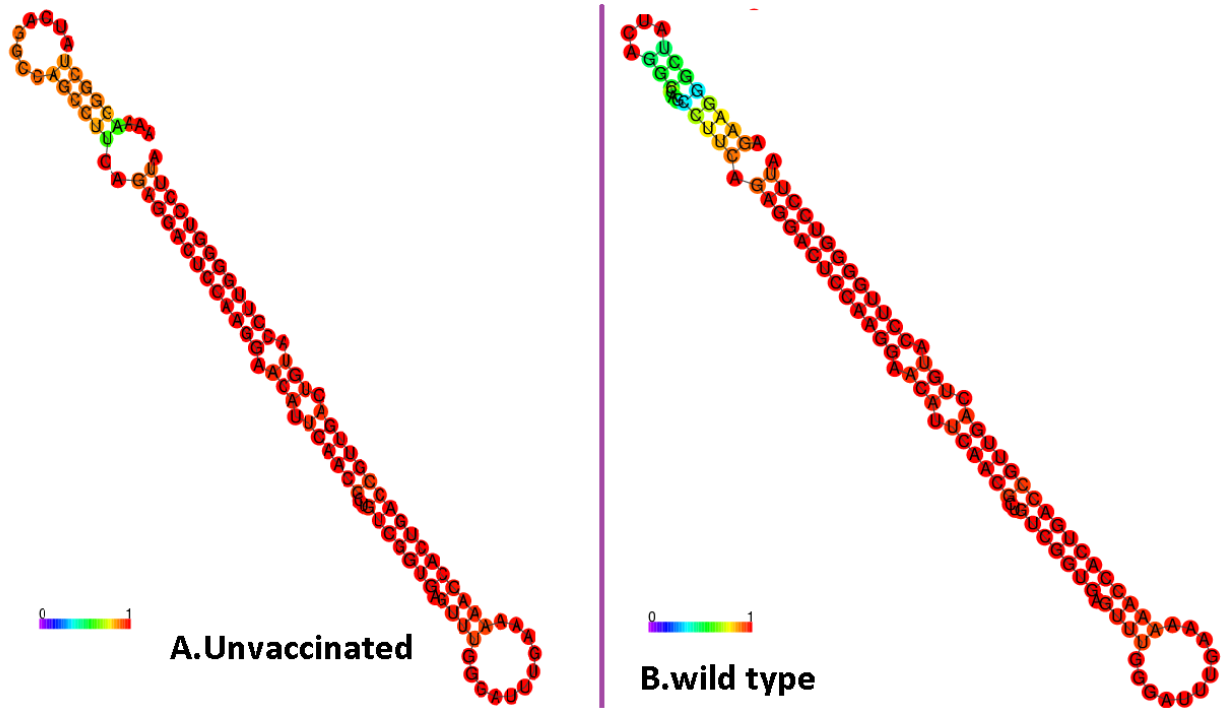

Figure 3.4 The secondary structure of hsa-mir-181a ACE2 is depicted graphically in the structure drawing, which encodes base-pair probabilities ranging from red (1% kcal/mol) to purple (0% kcal/mol). A. Sample 1 is unvaccinated with an MFE of -52.90 kcal/mol. **And** the thermodynamic ensemble is -**53.88**kcal/mole. **B**. Sample of wild type with a (MFE) of -**53.70** kcal/mole. The thermodynamic ensemble is -**54.75** kcal/mole.

The largest change that occurred in the (MFE) of the vaccinated samples was in sample number 11 where was with a (MFE) of -**47.00** kcal/mole. The thermodynamic ensemble is -**47.63** kcal/mole in Figure 3.5.

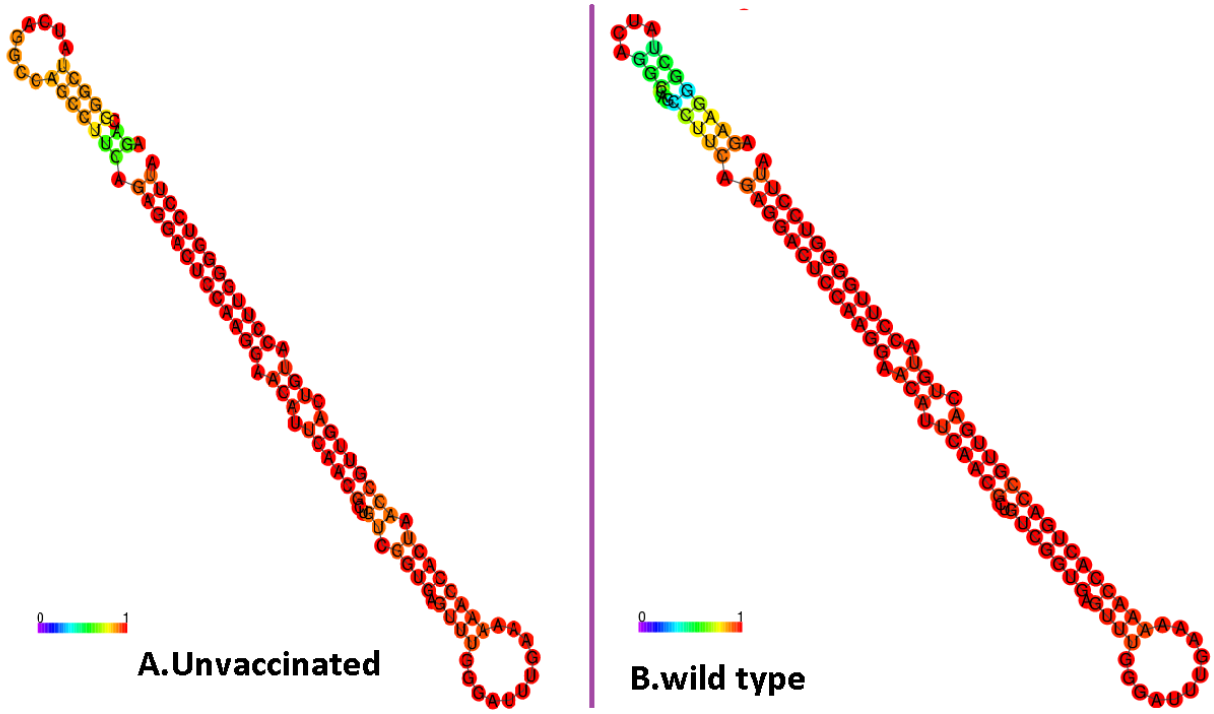

Figure 3.5 The Graphical drawing of secondary structure of *hsa-mir-181a ACE2* as in structure drawing encoding base-pair probabilities from red 1% to purple 0% kcal/mole. **A**. Sample 11 of unvaccinated with a (MFE) of -**47.00**kcal/mole. **And** the thermodynamic ensemble is -**47.63** kcal /mole. **B**. Sample of wild type with a (MFE) of -**53.70** kcal/mole. The thermodynamic ensemble is -**54.75** kcal/mole.

The optimal secondary structure in dot-bracket notation of universal sequences of all micro-RNA sequences of 20 unvaccinated samples as a multiple sequence alignment with a (MFE) of **75.99** kcal/mole (**47.86** plus **28.14** from covariance contributions) is given below. The thermodynamic ensemble is **76.74** kcal/mole as given below. Figure 3.6

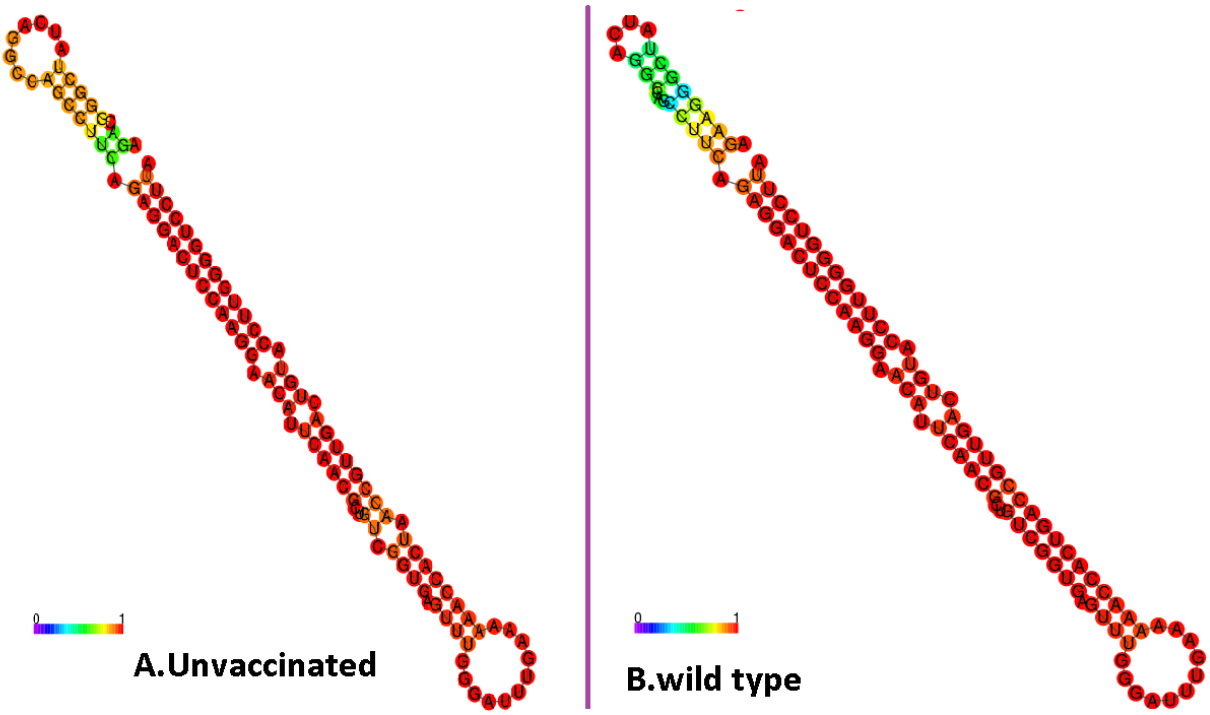

Figure 3.6 The secondary structure of hsa-mir-181a ACE2 is depicted graphically in the structure drawing, which encodes base-pair probabilities ranging from red (1% kcal/mol) to purple (0% kcal/mol). **A**. The multiple sequence alignment of all micro-RNA sequences of 20 unvaccinated samples with a (MFE) of -75.99 kcal/mole. The thermodynamic ensemble is -76.74 kcal /mole. **B.** Sample of wild type with a (MFE) of -53.70 kcal/mole. The thermodynamic ensemble is -54.75 kcal/mole.

Discussion

Through our study, we found a clear significant relationship in the effect of the vaccine on the change of the secondary structure of microRNA of hsa-mir-181a ACE2 depending on the value of (MFE) of the secondary structure of microRNA While the value (MFE) increased in the vaccinated comparative with unvaccinated, with a clear significant difference shown in figure 3.1 Also at the level of The thermodynamic, were an increase in vaccinated comparative with unvaccinated in where the difference was clear and the relationship was achieved in figure 3.2. This indicates that maybe the vaccine has a direct effect on the shape of the secondary structure of the microRNA, and since changing the secondary structure shape of the microRNA has an effective and important role in the gene expression of all types of genes, including hsa-mir-181a ACE2 gene. Which is the direct key to receiving the spike protein of the vaccine or COVID-19 this means that the vaccine may have a negative future role and is ineffective if it causes modifications in the gene expression of the cellular receptors. Due to the high prevalence of hsa-mir181a ACE2 in vaccinated and its association with higher chances of recurrence and poorer prognosis, we hypothesized that hsa-mir-181a is miRNA previously linked to ACE2 gene expirations and recurrence in humans, may be associated with the fusion gene.

Conclusion

The study of bioinformatics is one of the important studies for predicting genetic diagnosis and gene expression. RNAalifold web server were exploited to measure the amount of minimum free energy and dynamic thermodynamic energy of some biomolecules represented by micro-RNA and show the difference and effects on them by comparing the amount of the vaccinated and non-vaccinated types and comparing these amounts(minimum free energy and dynamic thermodynamic energy) with the wild type.

Acknowledgments

Feelings of love are renewed for everyone who contributed to opening another flower in the field of our achievement, which if it were not for them, would not exist.

Ethical statement

Permission and consent were taken from all participating patients.

Conflict of interest: None

References

1- Lai, X., Wolkenhauer, O., & Vera, J. (2016). Understanding microRNA-mediated gene regulatory networks through mathematical modelling. Nucleic acids research, 44(13), 6019-6035.

2- Yameny, A., Alabd, S., Mansor, M. MiRNA-122 association with TNF-α in some liver diseases of Egyptian patients. *Journal of Bioscience and Applied Research*, 2023; 9(4): 212-230. doi: 10.21608/jbaar.2023.329927

3- Alquraishi, M. K., & Alzeyadi, M. The effect of COVID-19 on micro RNA and therefore gene expression. International Journal of Health Sciences, (II), 5056-5062.

4- Cammaerts, S., Strazisar, M., De Rijk, P., & Del Favero, J. (2015). Genetic variants in microRNA genes: impact on microRNA expression, function, and disease. Frontiers in genetics, 6, 186.

5- Torday, J. S., & Miller, W. B. (2020). Cellular-molecular mechanisms in epigenetic evolutionary biology (pp. 19-28). Cham: Springer.

6- Ye, J., Xu, M., Tian, X., Cai, S., & Zeng, S. (2019). Research advances in the detection of miRNA. Journal of pharmaceutical analysis, 9(4), 217-226.

7- Alles, J., Fehlmann, T., Fischer, U., Backes, C., Galata, V., Minet, M., ... & Meese, E. (2019). An estimate of the total number of true human miRNAs. Nucleic acids research, 47(7), 3353-3364.

8- Mathews, D. H. (2019). How to benchmark RNA secondary structure prediction accuracy. Methods, 162, 60-67.

9- Martin, N. S., & Ahnert, S. E. (2022). Fast free-energy-based neutral set size estimates for the RNA genotype-phenotype map. Journal of the Royal Society Interface, 19(191), 20220072.

10- Sloma, M. F., Zuker, M., & Mathews, D. H. (2020). Predictive methods using RNA sequences. Bioinformatics, 155.

11- Alquraishi, M. K., & Alzeyadi, M. (2023). Bioinformatics Analysis of has-miR-181a in some COVID-19 Vaccinated People in Al-Najaf Province. Egyptian Academic Journal of Biological Sciences. C, Physiology and Molecular Biology, 15(2), 181-193.